Hindawi
International Journal of Polymer Science
Volume 2023, Article ID 1142654, 12 pages
https://doi.org/10.1155/2023/1142654

Research Article

Influence of Magnetic Wood on Mechanical and Electromagnetic Wave-Absorbing Properties of Polymer Composites

Satish Geeri,[1] **B. Krishna Murthy**,[2] **Aditya Kolakoti**,[3] **M. Murugan**,[4] **P. V. Elumalai**,[5] **N. R. Dhineshbabu**,[6] **and S. Prabhakar**[7]

[1]*Department of Mechanical Engineering, Pragati Engineering College, Surampalem, Andhra Pradesh 533437, India*
[2]*Department of Mechanical Engineering, Sasi Institute of Technology and Engineering, Tadepalligudem, Andhra Pradesh 534101, India*
[3]*Department of Mechanical Engineering, Raghu Engineering College, Dakamarri, Visakhapatnam, Andhra Pradesh 531162, India*
[4]*Department of Mechanical Engineering, Aditya College of Engineering and Technology, Surampalem, Andhra Pradesh 533437, India*
[5]*Department of Mechanical Engineering, Aditya Engineering College, Surampalem, India*
[6]*Department of ECE, Aditya Engineering College, Surampalem, India*
[7]*Department of Automotive Engineering, Wollo University-Kiot, Ethiopia*

Correspondence should be addressed to M. Murugan; murukar@gmail.com, P. V. Elumalai; elumalai@aec.edu.in, and S. Prabhakar; prabhakar@kiot.edu.et

Received 10 November 2022; Revised 10 January 2023; Accepted 11 January 2023; Published 1 February 2023

Academic Editor: Önder Pekcan

The application of wireless electronic devices is increasing nowadays; hence, there is a necessity for electromagnetic wave-absorbing material, which is mechanically stable. Polymer composites with magnetic wood as filler material were fabricated by hand lay-up methods of 6 mm thickness. For the proposed immersion duration, magnetic wood was developed by in situ chemical co-precipitation methods. The microwave absorbing phenomenon is evaluated based on the complex permeability, complex permittivity, dielectric tangent, and magnetic tangent losses. The experimentation was done by vector network analyzer in the frequency range of 8.2–12.4 GHz by X-band and Through-reflect-line (TRL) calibration. It was observed that the reflection losses increase as the immersion time increases from −8.70 dB to −9.30 dB at the frequency range of 10.2 GHz. A similar trend is also followed for the mechanical properties like tensile strength, bending strength, and impact strength with respect to the immersion time. The results revealed that the best mechanical and electromagnetic absorption properties are obtained for the specimens with immersion time of 72 hours. Validation is done for the electromagnetic wave-absorbing properties and mechanical properties by regression analysis, and the experimental data are in close agreement with the regression data.

1. Introduction

The usage of the wireless communication devices is escalating day by day, and also the rapid growth of electronic appliances leads to generate electromagnetic (EM) waves. These EM waves have an impact on human health and also on the durability of electronic instruments. Hence, there is a need to reduce the intensity of EM waves by using a shielding material. There are two different approaches for processing shielding material for EM waves, and the first one is that the material should absorb or reflect the EM waves when placed in specific applications. The second one is reinforcing the dielectric and magnetic particles in the material to act as a shielding material. Mechanical strength is also an essential parameter for this shielding material when placed in application [1–3]. The shielding material as a composite can be preferable, as the composites can be fabricated by involving the properties like dielectric and/or magnetic losses. Hence, these are influenced by the reflection losses (RLs), which reflect the EM wave's performance.

Table 1: Specification of composites.

S. no	Immersion time of oakwood in solution (hours)	No. of E-glass mat	Composites
1	24	3	Specimen 1
2	48	6	Specimen 2
3	72	9	Specimen 3

The fabrication process was done based on the second method, by adding magnetic wood to the polymer-based composites. Still, there is a requirement for EM wave-absorbing material with lightweight, more strength, and easy to process [1–4].

The works carried out for improving the absorbing properties of EM waves are by synthesis of magnetic wood [4], nanoparticles [5–7], and coated materials [8, 9]. Wood is a naturally available resource and degradable material; hence, there is a scope for research to be carried out on magnetic wood-based polymer composites to absorb the EM waves generated by wireless communication systems.

Even though these composites have some limitations as mentioned in the previous works, they are still used in many applications [10]. It has been proved that magnetic wood has strong magnetic properties of absorbing nature by Oka et al. [11–13]. The multi-layer magnetic composites were fabricated using in situ chemical co-precipitation method and followed by a hot pressing procedure. The EM wave-absorbing performance improved from −14.14 dB to −60.16 dB as the layers increased from 3 to 7 [14]. The EM absorbing properties were studied by in situ method with magnetic nanoparticles developed for poplar wood flours. The best results are obtained for different weight ratios of virgin wood floors and magnetic wood flours [15]. Depending on the thickness of the composites, the EM absorbing properties will be influenced [16].

The composites were fabricated based on the porous Fe_3O_4 decorated graphene, and the developed Fe_3O_4 decorated graphene specimens exhibit an enhanced dielectric loss [17]. Studies were carried out on magnetic CO Fe_3O_4 and hydroxylapatite through a hydrothermal process, and the results revealed that the specimen had improved mechanical properties. It is also concluded that these composites have influenced lift, drag, alignment, and actuation by magnetic fields [18]. The composites were fabricated with iron oxide with a facile hydrothermal method with ferric trichloride and ferrous chloride as the precursors at 90°C. It is concluded that these composites have strong absorbing nature of EM waves [19].

Oka et al. [20] investigated the properties of powder-type magnetic wood composites for different mixed ratios of Mn–Zn ferrite and Ni–Zn ferrite powder. The experimental data reveals that the mixed ratio influences by EM wave-absorbing properties and the thickness of the board [20]. Wang et al. [21] fabricated a lightweight with soft magnetic wood-based composites. It is stated that EM absorbing properties are influenced by the weight percentage of $FeNi_3$ [21].

Gao et al. [22] prepared a Fe_3O_4 wood composite by in situ chemosynthesis at room temperature by processing the specimen with X-ray powder diffraction (XRD), Value stream mapping (VSM), and Fourier transform infrared spectroscopy (FTIR) techniques. The results showed that the average grain size of Fe_3O_4 was approximately 14 nm. The vibrating sample magnetometry showed that the composites have saturation magnetisation M_s values from 4.7 to 25.3 emu/g, and concluded that interaction between wood and Fe_3O_4 turned stronger when less Fe_3O_4 was introduced in the composition [22].

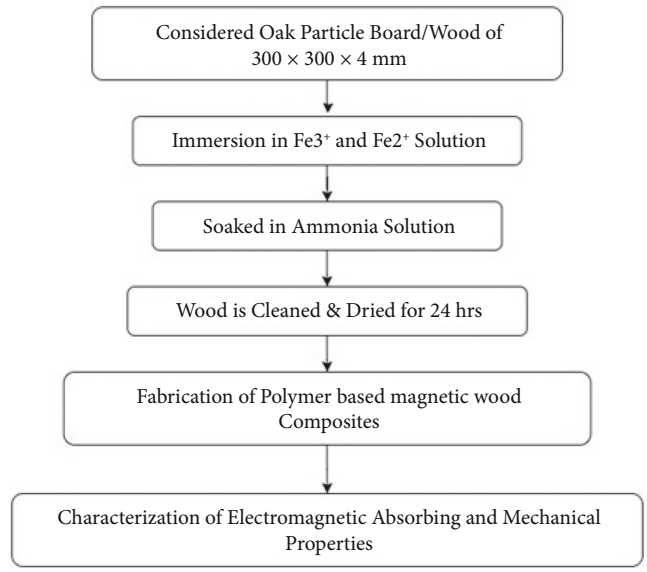

Figure 1: Flowchart of fabrication process.

Based on the above literature study, it is clear that only a few researchers reported on the hand lay-up technique in magnetic wood-based polymer composites. It was also observed that most of the works focused purely on EM wave-absorbing behaviour. But in the present work, an attempt has been made to improve the EM properties as well as mechanical strength. The experimental results have been validated with the regression analysis, and the values have high accuracy.

In the present work for the development of magnetic wood, the impregnated method is chosen [23], i.e., Fe^{2+} and Fe^{3+} solutions are used to immerse specimens. Hence, Fe_3O_4 particles were developed using the wood's in situ chemical reaction method [24]. The main aim of the fabricated composites should have a strong absorbing nature and more strength.

2. Experimental Details

2.1. Materials. The core region of the oak wood tree's main branch was considered a filler material for the present work. The other materials are epoxy resin (Aralide AW 106), E-glass fibre (woven fabric 310 gsm), and hardener (HV 953 U) with the required proportions were considered.

2.2. Synthesis of Magnetic Wood. Oak particleboard was considered to fabricate the composites with 300 × 300 × 5 mm dimensions for three proposed specimens. After washing with distilled water, it was immersed in the mixed solution 2 : 1 molar ratio of Fe^{3+} and Fe^{2+} solutions for 24 hours, 48

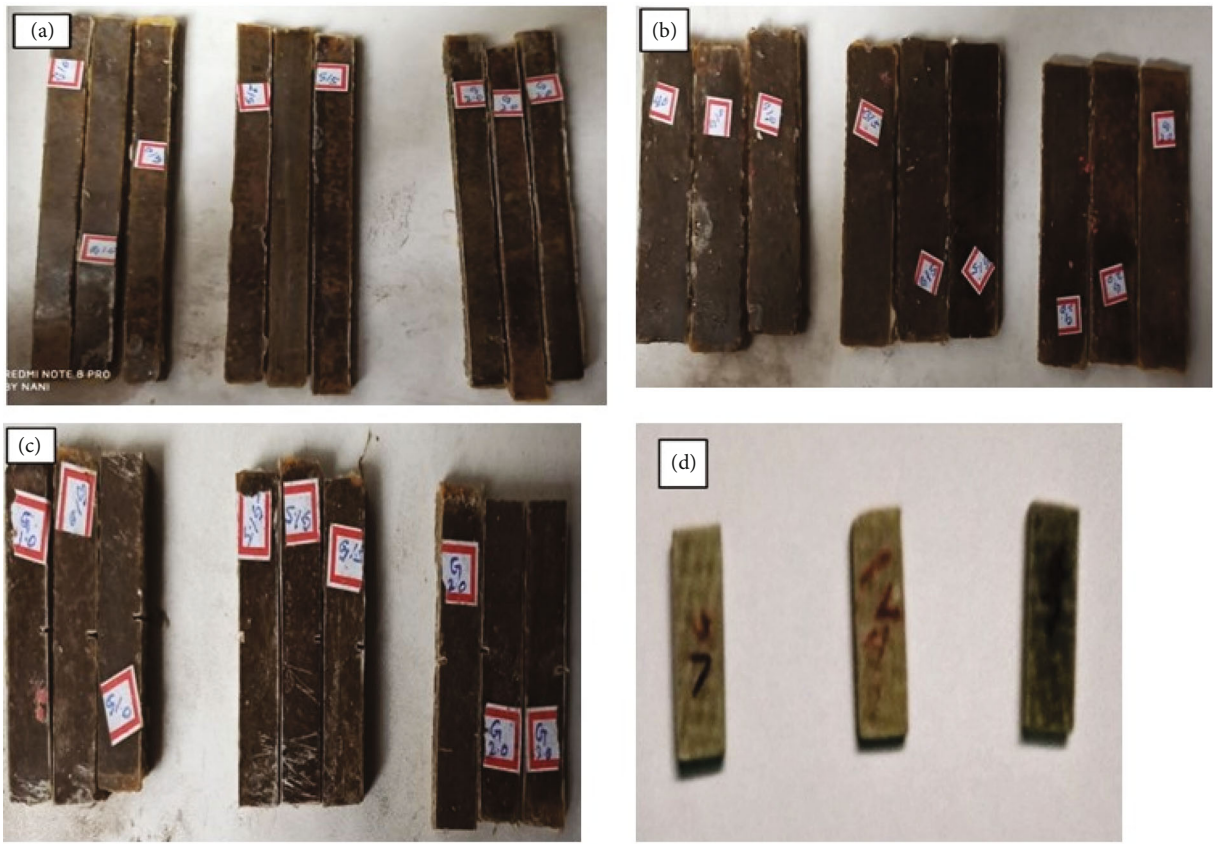

Figure 2: (a) Fabricated specimens for tensile testing, (b) fabricated specimens for bending testing, (c) fabricated specimens for impact testing, (d) fabricated specimens for electromagnetic wave-absorbing testing.

hours, and 72 hours at room temperature. Later, the three specimens are soaked in ammonia solution for the same duration and followed by cleaning with distilled water and drying in sunlight. As the immersion time increases, the thickness swelling also increases. After going through these stages, the wood appears like a light shade of red colour with partially semi-solids in nature. This is used as a filler material for these composites during the fabrication processes. The magnetic/oak wood is placed at the centre of the composites along with the specification, as shown in Table 1.

2.3. Fabrication of Magnetic Wood-Based Polymer Composites. The E-glass mat is placed one after the other for all three specimens with polymer as per the proposal. But, placing the magnetic/oak wood at the centre of composites with a sequence of order after 2nd, 3rd, and 5th glass mat for specimens 1, 2, and 3, respectively. A hand lay-up technique was chosen for the fabrication process for the proposed specimens, as shown in Figure 1. Finally, three composites were fabricated with 300 × 300 mm dimensions.

2.4. Characterization. The tensile test was done at room temperature on a universal testing machine based on American Society for Testing and Materials (ASTM) D 638-89 standards. The stiffness property was determined by conducting the flexural test on a universal testing machine with ASTM D 790-86 standards, and the impact test was performed using ASTM D 7136-15 standards. The mechanical properties were determined for the three specimens by choosing five different locations of each composite for experimentation, and the specimens are shown in Figures 2(a), 2(b), and 2(c). The specimens with the dimensions 22.86 × 10.16 mm were considered to evaluate the EM wave-absorbing properties by WR 90 waveguide method, and the specimens are as shown in Figure 2(d). These properties were calculated in the frequency range of 8.2–12.4 GHz with Through-reflect-line (TRL) calibration by a vector network analyzer (R&S ZVB 20). The EM wave-absorbing properties measure based on Equations (1) and (2).

$$\mathrm{RL_{dB}} = 20\,\mathrm{Log}_{10}\left(\frac{Z_i - Z_0}{Z_i + Z_0}\right), \tag{1}$$

$$Z = Z_0\sqrt{\frac{\mu_r}{\varepsilon_r}}\tanh\left(2\pi f\sqrt{\mu_r\varepsilon_r\mu_0\varepsilon_0}\times t\right). \tag{2}$$

Here Z_i is input impedance, Z_0 is absorber interface 377 Ω, f is the frequency in GHz, and $\varepsilon_r$and μ_r are relative complex permittivity and permeability, where space $\varepsilon_0 = 8.854 \times 10^{-12}$ F/m^{-1}, μ_r relative permeability of dielectric material, ε_r relative permittivity of magnetic material, t thickness, $\mu_0 = 4\Pi\times 10^{-7}$ H/m^{-1}.

2.5. Morphology of Composites. The SEM image of Figure 3(a) was taken after the tensile test conducted on

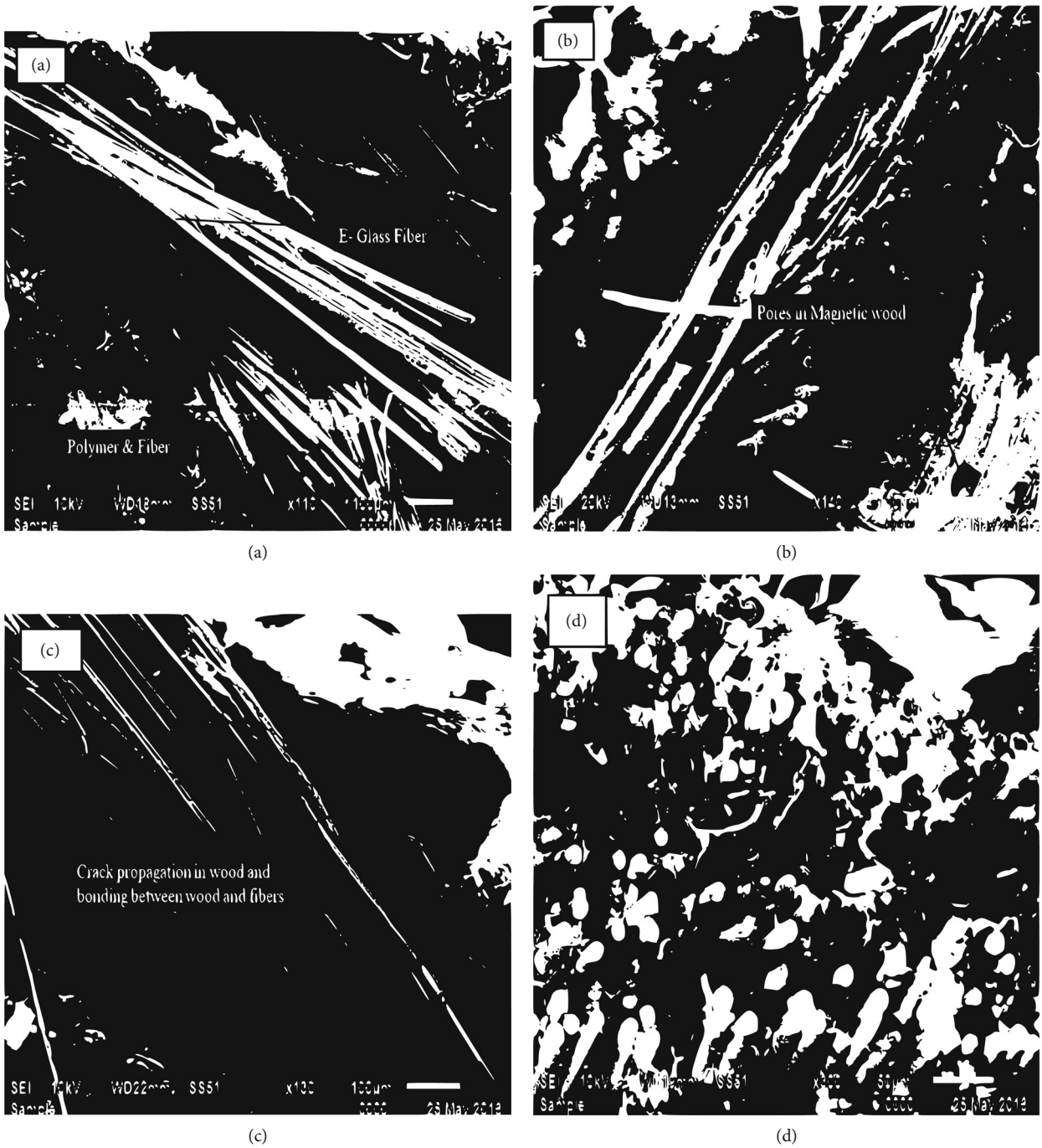

Figure 3: SEM image showing: (a) E-glass mat and polymer, (b) pores in wood, (c) the crack in wood and polymer, and (d) fibre pull-out from polymer.

composite, and it is evident that fibre is pulled out from the polymer as load acting in the fibre direction. As per the scanning electron microscope (SEM) images (Figure 3(a)), it is also evident that wood, polymer, and E-glass mats have a good bonding. During the magnetic treatment procedure, the specimen is placed in the solution for 24 hours, 48 hours, and 72 hours separately. Hence, the specimen colour, thickness, and state of nature (solid to semi-solid) changed. It is observed that the pores present in the wood are reduced after the magnetic treatment process, as the swelling in the specimen takes place, as shown in Figure 3(b). Due to the presence of pores in the wood/polymer, the stress transfer cannot occur uniformly, which leads to failure. The image in Figure 3(b) was taken from the flexural tested specimen.

It is also observed that as immersion time increases, the pores in the wood will reduce further. It has more impact on the performance of EM wave-absorbing nature, as shown in Figure 3(c). But at the same time, the presence of pores in wood/polymer material leads to failure of the specimen, as shown in Figure 3(c), and the particular wood has less strength.

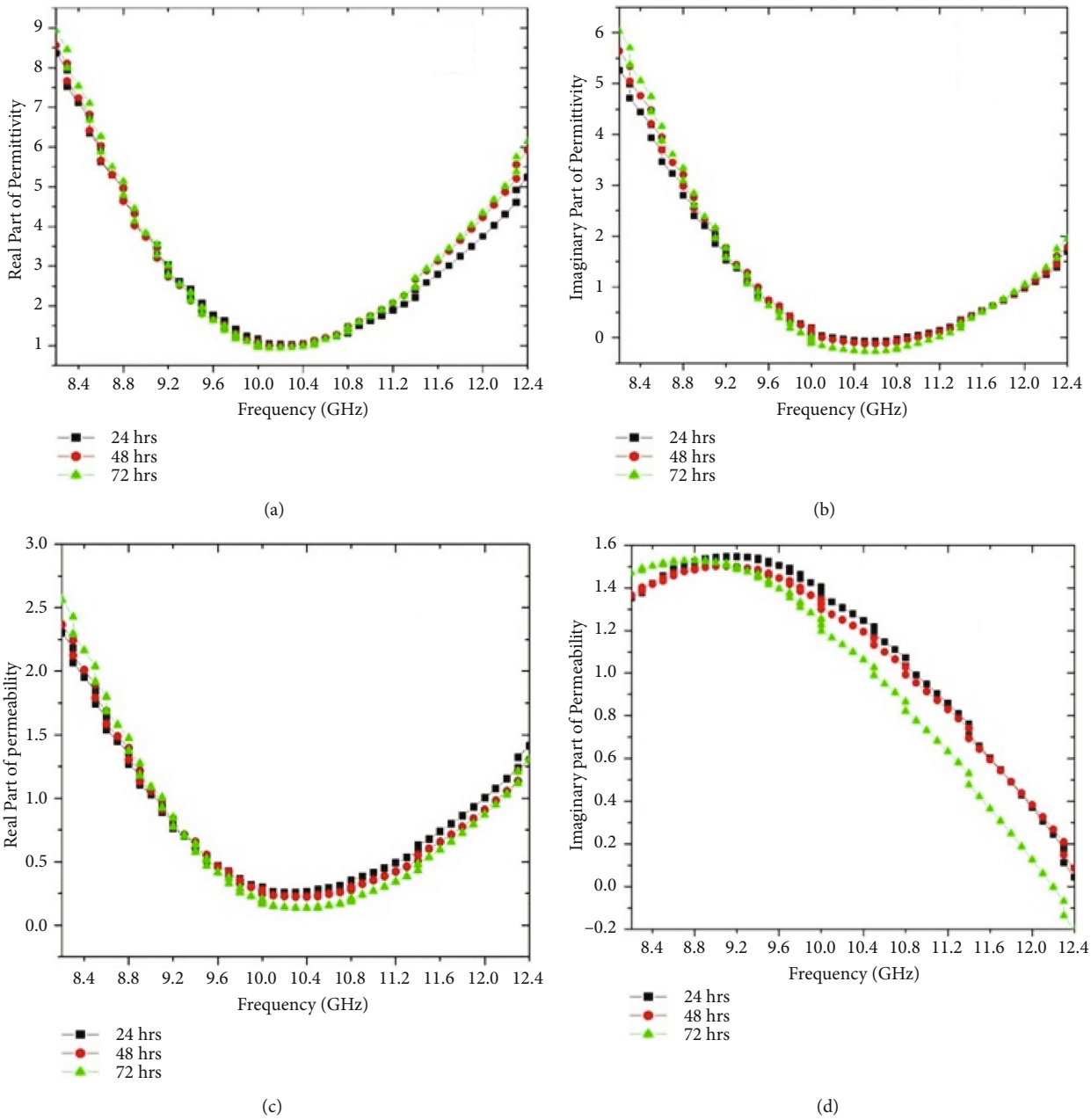

Figure 4: (a) Real part of permittivity, (b) imaginary part of permittivity, (c) real part of permeability, (d) imaginary part of permeability.

The crack propagation starts from the pores present in the wood; due to the acidic nature of ferrous chloride, ferric, and ammonia solution, there was partial decomposition of wood, and the shape/texture of wood changes. After the experimentation and the specimen from Figure 3(d), it is clear that the fibre is pulled out from the polymer material at the failure of the specimen.

3. Results and Discussions

An EM wave absorber is needed to protect humans and the environment. The polymer composites of EM wave-absorbing ability with stable mechanically are essential in the application. Based on Equations (1) and (2), the EM wave-absorbing properties were calculated in terms of relative complex permeability, relative complex permittivity, tangent losses, and RLs. After that, a morphological study is required to study the failure of the composites.

3.1. Electromagnetic Properties. The EM properties of wood-based composites have been evaluated experimentally by using a vector network analyzer with waveguide methods. The relative complex permittivity and permeability of composites are shown in Figure 4(a).

To investigate the EM wave-absorbing properties, it is essential to know the complex permittivity and permeability behaviour in the frequency range of 8.2–12.4 GHz by using

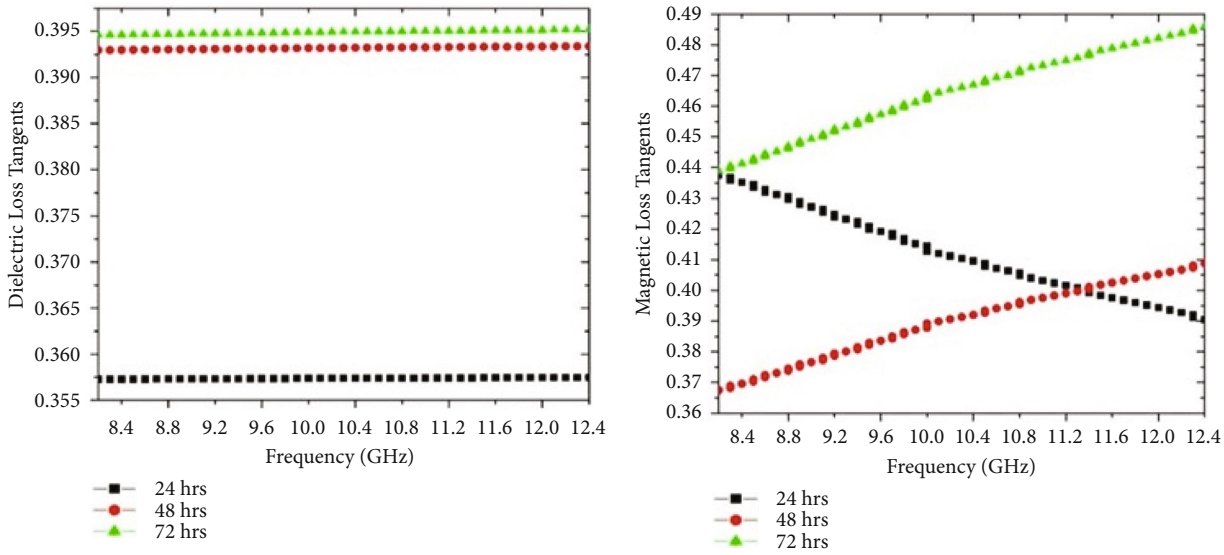

Figure 5: (a) Dielectric loss tangents, (b) magnetic loss tangents.

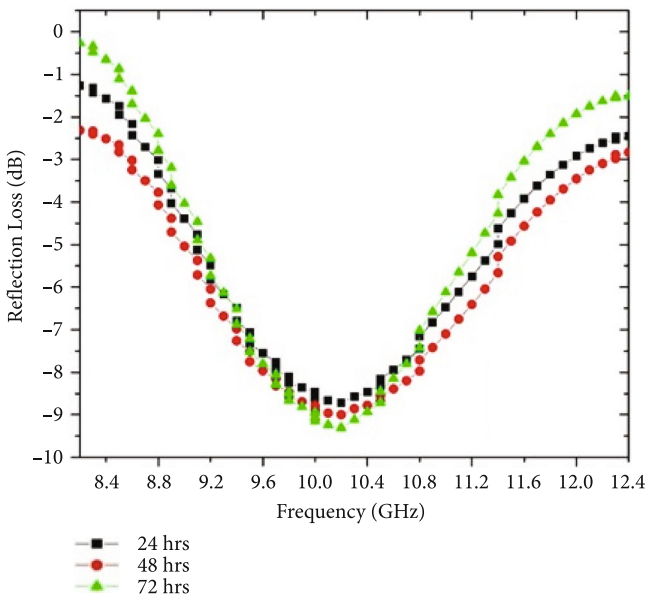

Figure 6: Reflection loss (RL).

Table 2: Reflection loss (RL) for different composites.

Submerged time (hours)	Absorbing peck (GHz)	Peck value (dB)	Band value (dB)
24	10.2	−8.70	−1.26
48	10.2	−8.99	−0.25
72	10.2	−9.40	−2.31

Equations (1) and (2). The real and imaginary part of complex permittivity represents the electric storage capability and loss capability [4]. These complex permittivity and permeability are generated from electronic polarization, ion polarization, intrinsic electric polarization, and magnetic properties and influence on the EM absorbing behaviour.

As the conductivity nature of samples gradually increases by increasing the submerged time of the samples from 24 hours to 72 hours, the specimens have the highest value in both real and imaginary part permittivity. Hence with the combination of good impedance matching behaviour and strong ability for EM attenuation, the absorbing nature is achieved for 72 hours submerged specimen [4, 25].

As shown in Figure 4(a), the real part of permittivity is improved as the immersion time of the specimen increases. The complex permittivity values are higher for the 72 hours submerged specimen due to the influence of electric polarization and electric conductivity. The chemical bonds have oxygen content when a function with the exterior surface of wood, –OH, and –CO– will develop electric dipolar polarization. This polarization mechanism depends on the different valances of ions availability and electron transfer between Fe^{3+} and Fe^{2+} ions position [26, 28, 29].

The trend followed in the graphs of the real and imaginary part of permittivity developed due to interfacing (interface polarization) between Fe_3O_4 cluster and the carbohydrates from the wood, as shown in Figures 4(a) and 4(b). Hence, due to the interference of polarization and dipole relaxation, there was an improvement in the EM properties [17, 29].

The fabricated composites show a strong magnetic loss in the frequency range, and the real part of permeability is more than the imaginary part of complex permeability. It is evident from Figures 4(c) and 4(d) that the real and imaginary part of complex magnetic permeability follows the same trend for the three specimens; as the immersion time increased, the permeability properties also improved.

It can be clearly seen that the real part of the permeability decreased up to 10.4 GHz and later increased at a higher frequency. Due to the impact of Fe^{3+} and Fe^{2+}ions in the

Table 3: The reflection losses compared with the literature.

Ref.	Filler material and method	Reflection losses and frequency	Present work
4	Oak wood and co-precipitation chemical interactions	−64.26 dB at 14.36 GHz	By co-precipitation chemical interactions for magnetic wood synthesis process and by hand lay-up method, the best results of RL are obtained at 10.2 GHz of −9.40 dB.
11	Wood and (1) coating type (Ni–Zn ferrite powder coated onto a fibre board), (2) powder type (Ni–Zn ferrite powder and cider wood powder mixed and pressed into boards), (3) impregnated type (cider wood impregnated with a water-based magnetic fluid), (4) sandwich type (combination structure consisting of a fibre board layer/magnetic binder layer/fibre board layer).	At 1.93 GHz, the RL as −16.69 dB, −13.83 dB, −3.64 dB.	
13	Coating-type magnetic wood	−14.56 dB at 10.0 GHz	
14	Oak wood and co-precipitation chemical interactions	−14.14 dB at 7 GHz	
20	Powder-type magnetic wood	−20 dB over the 2.5–6.2 GHz	

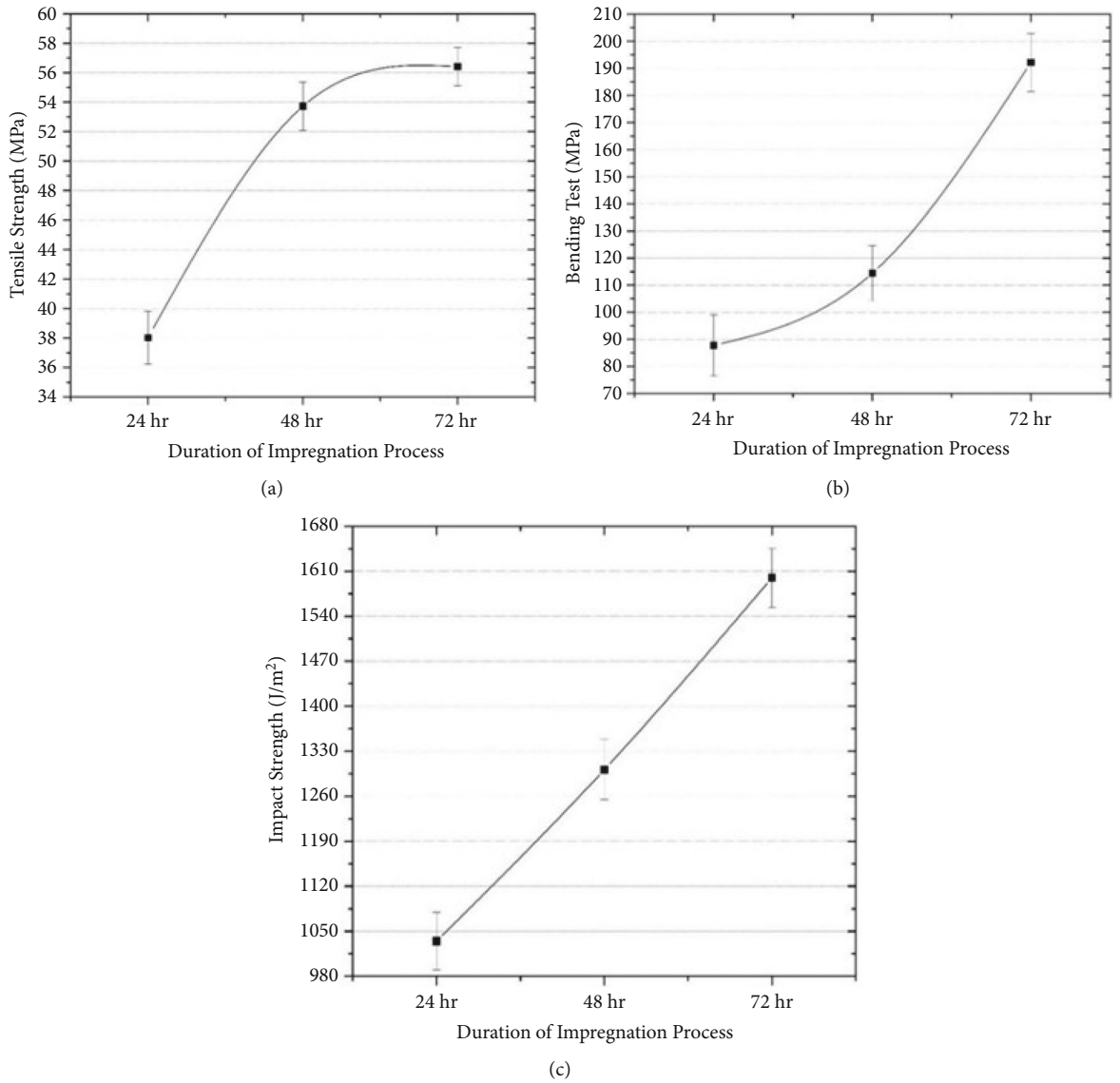

Figure 7: (a) Tensile strength for three different specimens, (b) bending strength for fabricated composites, (c) impact strength for fabricated composites.

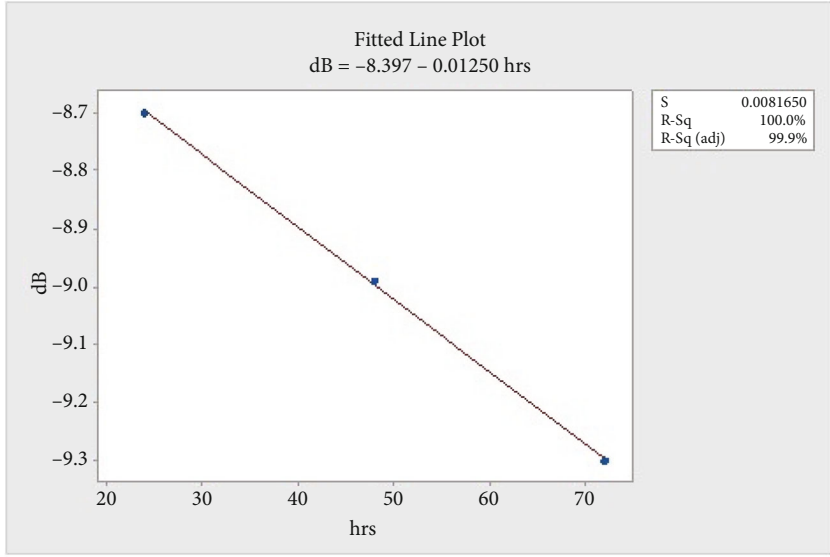

Figure 8: Fitted line plot of reflection loss.

wood, the real part of permeability increases above unity at a higher frequency and increases with increasing frequency. The imaginary part of permeability is close to zero in the frequency range of 9.6–12.4 GHz, as shown in Figure 4(d).

3.2. Tangent Losses by Dielectric and Magnetic Parameters. The absorbing nature of EM waves is usually influenced by the dielectric loss tangents and magnetic loss tangents [4]. Based on Figures 5(a) and 5(b), it is evident that the dielectric loss tangent value improves by the submerged time from 24 hours to 72 hours; a similar trend is followed for the magnetic loss tangent also. The magnetic loss tangent value for 72 hours submerged specimen has more RLs than the remaining specimens, and is increased with increasing frequency, as shown in Figures 5(a) and 5(b).

The 72 hours submerged specimen has the highest loss tangent value of 0.44 at 8.2 GHz and goes on to improve in the frequency range. Hence, it is the highest ability to convert the EM wave to energy in other forms, which is essential in EM wave-absorbing properties. Based on Figures 5(a) and 5(b), it is clear that the major contribution of magnetic parameter develops the EM wave-absorbing property then dielectric tangent loss due to eddy current loss [17, 29].

Based on Figure 5(a), the dielectric loss tangents are constant throughout the frequency range and are increased by increasing the submerged time. These losses are developed by having more content of Fe_3O_4 as conductive nature in the specimens.

3.3. Microwave Absorbing Properties. The RLs depend on parameters like filler material, the thickness of composites, the number of layers, etc. In the present work, wood-based polymer was present. Figure 6 shows magnetic wood-based polymer composites' measured/calculated RL properties for different submerged times.

It is clear that, as the submerged time increased, the EM wave-absorbing nature also improved from 24 hours to 72 hours at the frequency range from 8.2 GHz to 12.4 GHz, respectively. Many existing works on magnetic wood-based composites will have 90% attenuation of EM wave, and wide absorbing bandwidth was attained when the |RL| is more than 10 dB [4, 26, 29]. From Figure 6 and Table 2, it is evident that the RL values are close to 10 dB.

The magnetic property was developed in the composites due to iron salt impregnation duration of 24 hours, 48 hours, and 72 hours. It is clear that the submerged time influences on the EM wave-absorbing ability. As the submerged time increases, a sharp improvement in RL is noticed as it affects EM wave-absorbing nature. This behaviour is achieved due to the well-ordered structure of Fe_3O_4, which is in good agreement with research [25, 17, 29], and present results are compared with the previous works as reflected in Table 3.

4. Mechanical Properties

The objective of the present work is to have both EM wave-absorbing properties and good mechanical properties for the fabricated composites. With reference to Table 1, developing the good mechanical properties for the composites is done with two parameters: one by increasing the E-glass mat and the second by submerging process where the moisture amount is increased. As oak wood is immersed in the solution for 24 hours, 48 hours, and 72 hours, the moisture content significantly affects the composites' mechanical performance. For the fabricated composites, the tensile, bending, and impact tests were conducted as per the ASTM standards [30].

Based on the tensile strength, the basic information about the behaviour of the composites can be known. It is observed from Figure 7(a) that the tensile strength gradually increased from specimen 1 to specimen 3. Specimen 2 is improved by 41.25% compared to specimen 1 and similarly, specimen 3 is enhanced by 5% compared to specimen 2. The strength gradually improved from specimen 1 to 3 due to the improved stage of stress transfer ability between wood, E-

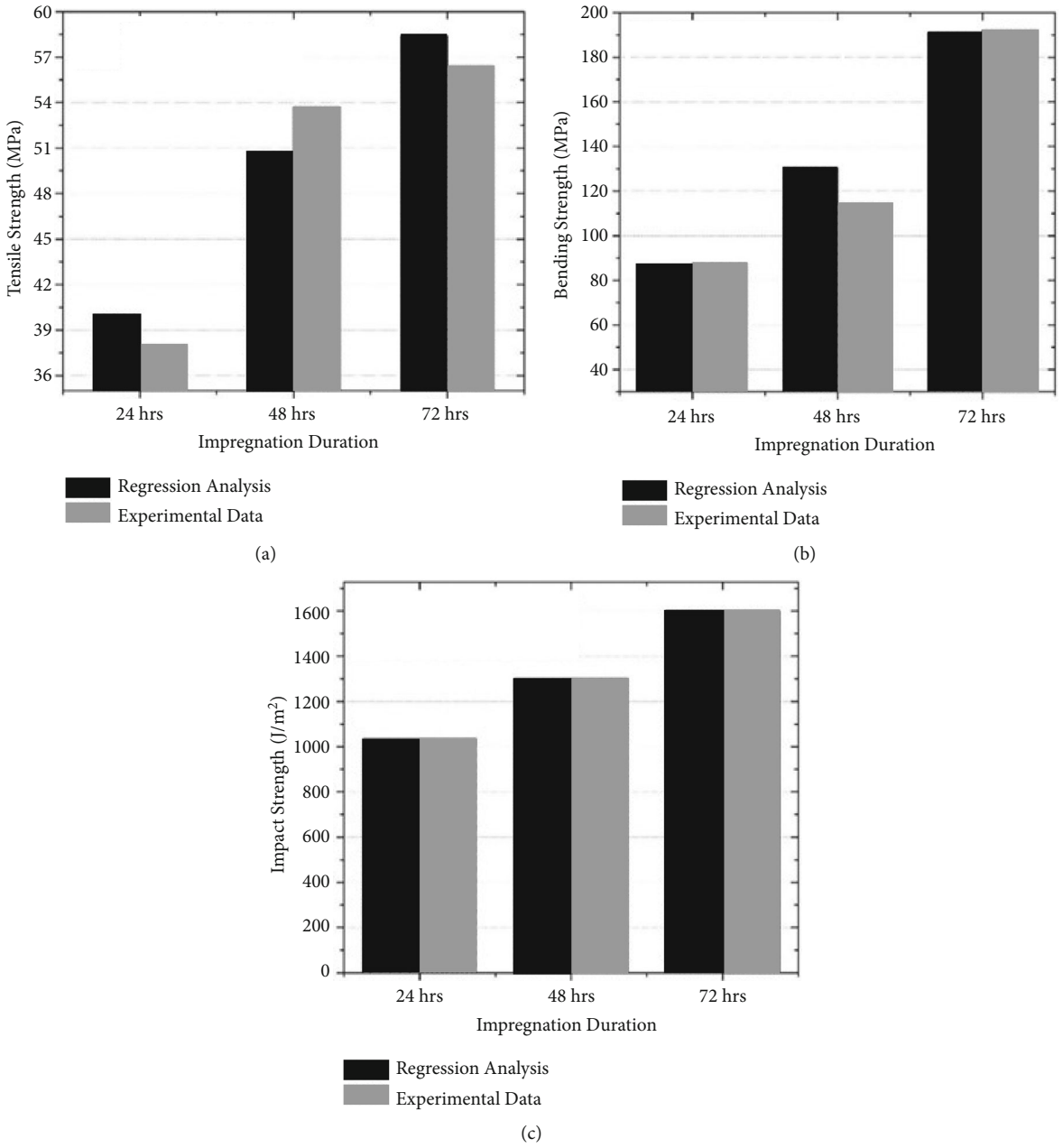

Figure 9: (a) Comparison of regression data and experimental data for tensile strength, (b) comparison of regression data and experimental data for bending strength, (c) comparison of regression data and experimental data for impact strength.

glass mat, and polymer. The improvement in the tensile strength occurs mainly for two reasons, i.e., one by increasing the number of E-glass mats from specimen 1 to 3, and warp fibres in composites are more in number to the direction of applied load in the universal testing machine [31–32]. The second reason is for having good bonding between polymer and wood, as shown in Figure 7(b). Hence, this study can conclude that wood filler-based polymer composites also exhibit a maximum tensile stress value.

Among the three specimens, specimen 3 has more stiffness, as represented in Figure 7(b). Specimen 2 is improved by 30.38% strength with reference to specimen 1, and the flexural strength of specimen 3 is improved by 68.05% compared to the previous specimen. The improvement was observed due to the following reasons. A more significant number of warp fibres are aligned along the specimen's longitudinal direction; to these fibres, the load is applied in the transverse direction. By increasing the number of E-glass mats also, more stiffness is developed in specimen 3 compared with other specimens.

A similar trend is followed in the case of the impact strength also. Specimen 2 is improved by 25.77%, and specimen 3 is improved by 22.95% compared to the previous specimens, as shown in Figure 7(c). As the bending strength and impact strength improve from specimen 1 to 3, it is clear that the composites have the capability to transfer the stress between matrix and filler. Hence, this leads to improvement in mechanical

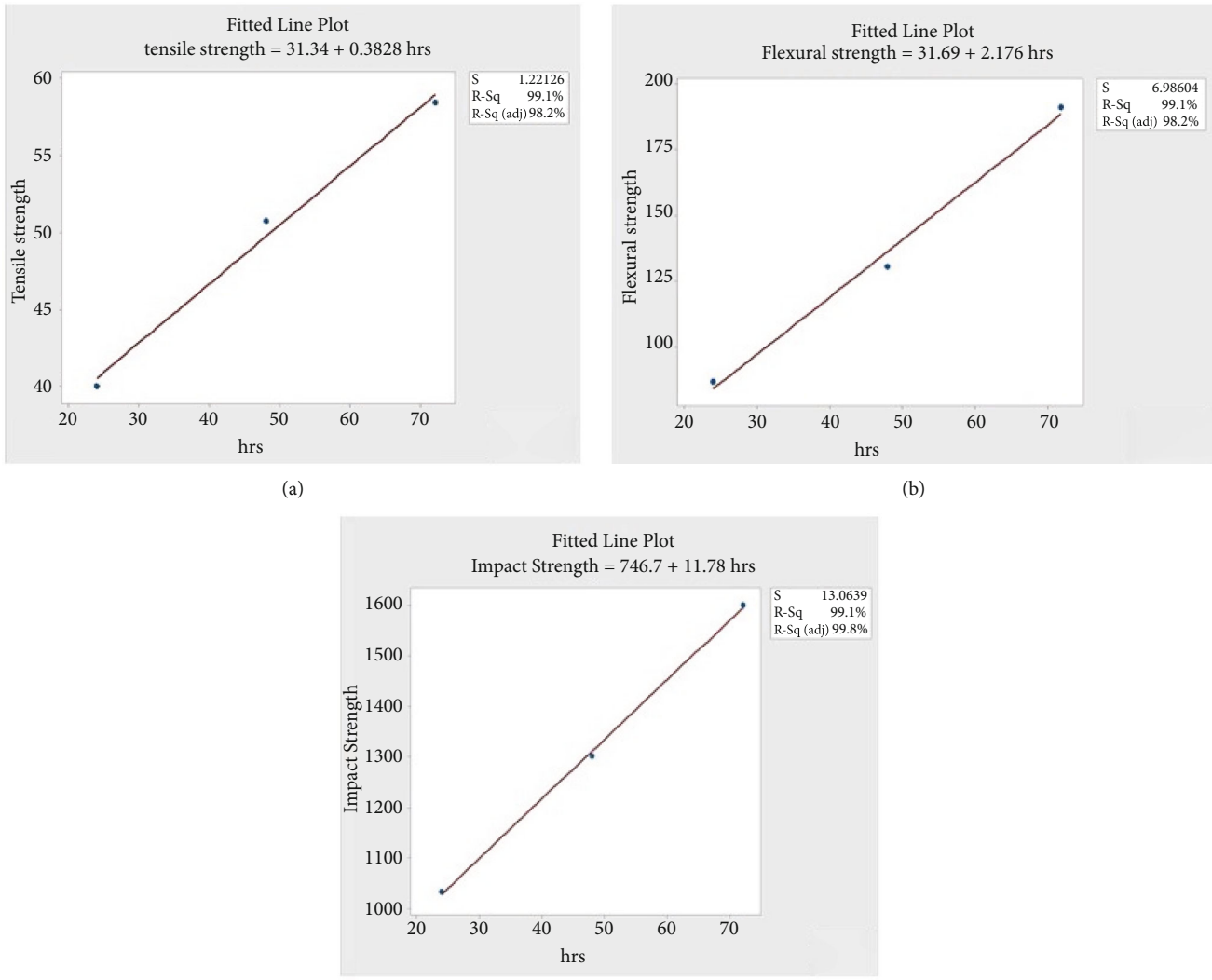

Figure 10: (a) Tensile strength data fitted to line, regression equation and R^2 value, (b) bending strength data fitted to line, regression equation and R^2 value, (c) impact strength data fitted to line, regression equation and R^2 value.

Table 4: Regression equation for mechanical properties.

Mechanical properties	Regression equation	R^2 value
Tensile strength	Tensile strength = 31.34 + 0.3828 immersion time	0.991
Bending strength	Bending strength = 31.69 + 2.176 immersion time	0.991
Impact strength	Impact strength = 746.7 + 11.78 immersion time	0.999

properties. It can be stated that the moisture present in the polymer composites impacts the mechanical properties.

5. Regression Analysis

Regression analysis is one of the simple techniques for finding the functional relationship among the variables and the influence of the variables on the response. The relation between the variables and the response will be generated based on the equation. In the present work, the input variables reflect losses and mechanical properties. In that process, the regression equation was developed for tensile strength, flexural strength, hardness, and EM wave-absorbing properties.

5.1. Development of Regression Equation for Electromagnetic Wave Absorption Properties. Based on Figure 8, it is clear that the experimental data is very close to the regression data and with high accuracy ($R^2 = 100\%$). The Equation (3) is generated for experimental data based on regression analysis, with immersion time as the input parameter and RL as the output parameter. The proposed regression

equation for RL has been predicted and valued with 100% accuracy to experimental data.

$$\text{Reflection loss (dB)} = -8.3967 - 0.012500\,\text{immersion time (hours)}, \quad (3)$$

5.2. Development of Regression Equation for Mechanical Properties. The experimental data are compared to the regression data and it is noticed that both are in good agreement, as shown in Figures 9(a), 9(b), and 9(c). The error in the experimental data is also calculated and significantly less based on the R^2 value. R^2 is approximately close to 99.1%, which indicates that the accuracy level is more for the experimental data, as represented in Figures 10(a), 10(b), and 10(c).

Based on Table 4, the equations were generated for experimental data by regression analysis with immersion time as input parameter and mechanical properties (tensile strength, bending strength, and impact strength) as output parameter. The proposed regression equations for mechanical properties have been predicted and valued with 99% accuracy to experimental data.

6. Conclusion

Polymer-based composites with magnetic wood by hand lay-up method have been proposed to study the mechanical and EM absorbing properties. The EM absorbing phenomenon was investigated in terms of RL for a different submerged time of specimen. The mechanical behaviour was also studied for specimens as the moisture content absorbed and increased the number of E-glass mats as the influencing parameters. From the results, the following findings have been derived.

The EM wave-absorbing properties are increased with an increase in the submerged period (24–72 hours) of wood. It is predicted that 72 hours submerged wood specimen has the maximum absorbing capability in X-band. The highest RL value of −9.40 dB is obtained at 10.2 GHz for specimen 3 due to the well-ordered structure of Fe_3O_4. The tensile strength is improved by 48.31% compared with specimen 1. This is the fact that good bonding between filler and matrix materials. Due to an increase in the number of E-glass mats and bonding parameters, the flexural strength is improved by 90% compared to specimen 1.The impact strength is increased by 54.64% due to moisture content absorbed and the bond between polymer and glass fibres. By the SEM image, it is clear about the failure analysis of composites. The experimental data (EM absorbing behaviour and mechanical properties) are very close to the regression data and are in good agreement with 99% accuracy.

Data Availability

On reasonable request, the data used in this research can be shared.

Conflicts of Interest

The author(s) declare that they have no conflicts of interest.

Authors' Contributions

Author SG, PS carried out the experimental investigations and wrote the first draft of the manuscript. BKM conducted experiments for various conditions. AK prepared the samples and contributed to write result and discussion part. MM coordinated with all authors and wrote the final draft of the manuscript and approved the same. PVE carried out detailed literature reviews related to the proposed work.

References

[1] T. Zhang, J. Zhang, H. Luo et al., "Facile approach to fabricate BCN/Fe-x(B/C/N)(y) nano-architectures with enhanced electromagnetic wave absorption," *Nanotechnology*, vol. 29, pp. 1–27, 2018.

[2] H. Lv, Z. Yang, P. L. Wang et al., "A voltage-boosting strategy enabling a low-frequency, flexible electromagnetic wave absorption device," *Advanced Materials*, vol. 30, no. 15, p. e1706343, 2018.

[3] M. Qiao, X. Lei, Y. Ma et al., "Application of yolk–shell Fe_3O_4@N-doped carbon nanochains as highly effective microwave-absorption material," *Nano Research*, vol. 11, no. 3, pp. 1500–1519, 2018.

[4] Z. Lou, H. Han, M. Zhou et al., "Synthesis of magnetic wood with excellent and tunable electromagnetic wave-absorbing properties by a facile vacuum/pressure impregnation method," *ACS Sustainable Chemistry & Engineering*, vol. 6, no. 1, pp. 1000–1008, 2018.

[5] S. E. Jacobo, J. C. Aphesteguy, R. Lopez Anton, N. N. Schegoleva, and G. V. Kurlyandskaya, "Influence of the preparation procedure on the properties of polyaniline based magnetic composites," *European Polymer Journal*, vol. 43, no. 4, pp. 1333–1346, 2007.

[6] I. Kong, S. H. Ahmad, M. H. Abdullah, D. Hui, A. N. Yusoff, and D. Puryanti, "Magnetic and microwave absorbing properties of magnetite-thermoplastic natural rubber nanocomposites," *Journal of Magnetism and Magnetic Materials*, vol. 322, no. 21, pp. 3401–3409, 2010.

[7] W. Bouzidi, N. Mliki, and L. Bessais, "Structural and magnetic properties of new uniaxial nanocrystalline Pr_5Co_{19} compound," *Journal of Magnetism and Magnetic Materials*, vol. 441, pp. 566–571, 2017.

[8] H. Garcia-Miquel, J. Carbonell, and J. Sanchez-Dehesa, "Modulation of electromagnic waves by alternating currents through left-handed ferromagnetic microwires," *Journal of Applied Physics*, vol. 111, no. 6, p. 63901, 2012.

[9] J. Carbonell, H. Garcia-Miquel, and J. Sanchez-Dehesa, "Double negative metamaterials based on ferromagnetic microwires," *Physical Review B*, vol. 81, no. 2, 2010.

[10] Z. Lou, Y. Zhang, M. Zhou et al., "Synthesis of magnetic wood fiber board and corresponding multi-layer magnetic composite board, with electromagnetic wave absorbing properties," *Nanomaterials*, vol. 8, no. 6, pp. 441–448, 2018.

[11] H. Oka, K. Narita, H. Osada, and K. Seki, "Experimental results on indoor electromagnetic wave absorber using

magnetic wood," *Journal of Applied Physics*, vol. 91, no. 10, pp. 7008–7010, 2002.

[12] H. Oka, K. Tanaka, H. Osada, K. Kubota, and F. P. Dawson, "Study of electromagnetic wave absorption characteristics and component parameters of laminated-type magnetic wood with stainless steel and ferrite powder for use as building materials," *Journal of Applied Physics*, vol. 105, no. 7, p. 7E701, 2009.

[13] H. Oka, Y. Kataoka, H. Osada, Y. Aruga, and F. Izumida, "Experimental study on electromagnetic wave absorbing control of coating-type magnetic wood using a grooving process," *Journal of Magnetism and Magnetic Materials*, vol. 310, no. 2, pp. E1028–E1029, 2007.

[14] L. Zhichao, Y. Zhang, Z. Ming et al., "Synthesis of magnetic wood fibre board and corresponding multi-layer magnetic composite board, with electromagnetic wave absorbing properties," *Nanomaterials*, vol. 441, pp. 1–14, 2018.

[15] M. Mashkour and Y. Ranjbar, "Superparamagnetic Fe_3O_4@ wood flour/polypropylene nanocomposites: physical and mechanical properties," *Industrial Crops and Products*, vol. 111, pp. 47–54, 2018.

[16] Y. Zheng, Y. Song, T. Gao et al., "Lightweight and Hydrophobic Three-Dimensional Wood-Derived Anisotropic Magnetic Porous Carbon for Highly Efficient Electromagnetic Interference Shielding," *ACS Applied Materials & Interfaces*, vol. 12, no. 36, pp. 40802–40814, 2020.

[17] S. Danping, Z. Quan, G. Qian, S. Chen, W. Jiang, and L. Fengsheng, "Controlled synthesis of porous Fe_3O_4-decorated graphene with extraordinary electromagnetic wave absorption properties," *Acta Materialia*, vol. 30, p. 30, 2013.

[18] W. Gan, L. Gao, X. Zhan, and J. Li, "Hydrothermal synthesis of magnetic wood and improved wood properties by precipitation with $CoFe_2O_4$/hydroxyapatitie," *RSC Advances*, vol. 5, pp. 45919–45927, 2015.

[19] W. Gan, L. Ying, Likun, Z. Xianxu, and J. Li, "Magnetic property, thermal stability, UV-resistance and moisture absorption behaviour of magnetic wood," *Polymer Composites*, vol. 38, no. 8, pp. 2–18, 2015.

[20] H. Oka, H. Osada, Y. Namiazki, and F. P. Dawson, "Electromagnetic wave absorption characteristics adjustment method of recycled powder-type magnetic wood for use as a building material," *IEEE*, vol. 48, p. 11, 2012.

[21] L. Wang, N. Li, Z. Tiqi, B. Li, and Y. Ji, "Magnetic properties of $FeNi_3$ nanoparticle modified Pinus radiata wood nanocomposites," *Polymers*, vol. 11, no. 3, pp. 421–426, 2019.

[22] H. L. Gao, G. Y. Wu, H. T. Guan, and G. L. Zhang, "In situ preparation and magnetic properties of Fe_3O_4/wood composite," *Materials and Technologies*, vol. 27, pp. 101–103, 2012.

[23] Y. Dong, Y. Yan, Y. Zhang, S. Zhang, and J. Li, "Combined treatment for conversion of fast-growing poplar wood to magnetic wood with high dimensional stability," *Wood Science and Technology*, vol. 50, no. 3, pp. 503–517, 2016.

[24] H. Oka, A. Hojo, K. Seki, and T. Takashiba, "Wood construction and magnetic characteristics of impregnated type magnetic wood," *Journal of Magnetism and Magnetic Materials*, vol. 239, no. 3, pp. 617–619, 2002.

[25] G. Sun, B. Dong, M. Cao, B. Wei, and C. Hu, "Hierarchical dendrite-like magnetic materials of Fe_3O_4, γ-Fe_2O_3, and Fe with high performance of microwave absorption," *Chemistry of Materials*, vol. 23, no. 6, pp. 1587–1593, 2011.

[26] H.-L. Xu, H. Bi, and Yang, "Enhanced microwave absorption property of bowl-like Fe_3O_4 hollow spheres/reduced graphene oxide composites," *Journal of Applied Physics*, vol. 111, no. 7, p. 7A522, 2012.

[27] S. Xie, Y. Yang, G. Hou, J. Wang, and Z. Ji, "Development of layer structured wave absorbing mineral wool boards for indoor electromagnetic radiation protection," *Journal of Building Engineering*, vol. 5, pp. 79–85, 2016.

[28] A. N. Yusoff, M. H. Abdullah, S. H. Ahmad, S. F. Jusoh, A. A. Mansor, and S. A. A. Hamid, "Electromagnetic and absorption properties of some microwave absorbers," *Journal of Applied Physics*, vol. 92, no. 2, pp. 876–882, 2002.

[29] C. Gao, X. He, F. Ye, S. Wang, and G. Zhang, "Electromagnetic wave absorption and mechanical properties of CNTs@GN@Fe_3O_4/PU multilayer composite foam," *Materials*, vol. 14, no. 23, pp. 7244–7250, 2021.

[30] P. V. Elumalai, N. R. Dhineshbabu, P. Varsala et al., "Effects of asna fibre reinforced with epoxy resin with and without steel wire mesh and simulation of car bumper," *Materials Research Express*, vol. 9, no. 5, p. 55301, 2022.

[31] D. babu, N. Raman, N. Mahadevi, and D. Assein, "Electronic applications of multi-walled carbon nanotubes in polymers: a short review," *Materials Today: Proceedings*, vol. 33, no. 1, pp. 382–386, 2020.

[32] V. Rajendran, N. R. Dhineshbabu, R. R. Kanna, and K. V. I. S. Kaler, "Enhancement of thermal stability, flame retardancy, and antimicrobial properties of cotton fabrics functionalized by inorganic nanocomposites," *Industrial and Engineering Chemistry Research*, vol. 53, no. 50, pp. 19512–19524, 2014.